Check for
updates

Towards Uniform Online Spherical Tessellations

Paul C. Bell[1] · **Igor Potapov**[2]

Abstract

The problem of uniformly placing N points onto a sphere finds applications in many areas. For example, points on the sphere correspond to unit quaternions as well as to the group of rotations SO(3) and the online version of generating uniform rotations (known as "incremental generation") plays a crucial role in a large number of engineering applications ranging from robotics and aeronautics to computer graphics. An online version of this problem was recently studied with respect to the *gap ratio* as a measure of uniformity. The first online algorithm of Chen et al. was upper-bounded by 5.99 and later improved to 3.69, which is achieved by considering a circumscribed dodecahedron followed by a recursive decomposition of each face. In this paper we provide a more efficient tessellation technique based on the regular icosahedron, which improves the upper-bound for the online version of this problem, decreasing it to approximately 2.84. Moreover, we show that the lower bound for the gap ratio of placing at least three points is $(1 + \sqrt{5})/2 \approx 1.618$ and for at least four points is no less than 1.726.

Keywords Online algorithms · Discrepancy theory · Spherical trigonometry · Uniform point placement · Computational geometry

Paul C. Bell
p.c.bell@ljmu.ac.uk

Igor Potapov
potapov@liverpool.ac.uk

1   School of Computer Science and Mathematics, Liverpool John Moores University, James Parsons Building, Byrom Street, Liverpool, Merseyside L3-3AF, UK

2   Department of Computer Science, University of Liverpool, Ashton Building, Ashton Street, Liverpool, Merseyside L69-3BX, UK

🖄 Springer

1 Introduction

One of the central problems of classical discrepancy theory is to maximise the uniformity of distributing a set of n points into some metric space [7]. For example, this includes questions about arranging points over a unit cube in a d-dimensional space, a polyhedral region, a sphere, a torus or even over a hyperbolic plane, etc. Applications of modern day discrepancy theory include those in viral morphology, crystallography, molecular structure, electrostatics, computing quadrature formulas [17], 3D projection reconstruction of Magnetic Resonance Images (MRI) [13], investigations of carbon fullerenes (C_{60} and C_{70}) [9], complexity theory [22], connections to quaternion rotations [3], Ramsey theory, problems in numerical integration, financial calculations, computer graphics, and computational physics [15]. The choice of discrepancy measure impacts the type of questions that can be studied. For example, a logarithmic variant of the Coulomb potential allows one to define Smale's 7th problem [20]; from a list of 18 important questions for the 21st century.

In order to measure the discrepancy from uniformity, the *gap ratio* metric was introduced by Teramoto et al. [23] for analysing dynamic discrepancy, i.e., the ratio between the maximum and minimal gap, where the maximum gap is the diameter of the largest empty circle on the sphere surface and the minimal gap is the minimum pairwise distance on the sphere surface (orthodromic distance). A similar measure of taking the radius of the largest empty circle over minimum pairwise distance is known as the "mesh ratio" [5] or "mesh-separation ratio" [6, 10]. One might consider defining uniformity just by measuring the closest two points, however this does not take into account large undesirable gaps that may be present in the point set. Alternatively one may use the standard measure from discrepancy theory; define some fixed geometric shape R and count the number of inserted points that are contained in R, whilst moving it all over some space. This measure has two main disadvantages—that of computational hardness of calculating the discrepancy at each stage and also that we must decide upon a given shape R, each of which may give different results [23]. Finally we mention the related "covering radius" for a given set of points which denotes the minimal sized radius such that spheres centred at these points cover the whole metric space (although we may note that such a discrepancy does not penalise two points which are close together); see [11] for a good introduction.

Generating a set of uniformity distributed points in non-Euclidean space is even more challenging and somewhat counterintuitive. For example, the problem of generating a point set on the 2-sphere which minimises criteria such as energy functions, discrepancy, dispersion and mutual distances has been extensively studied in the offline setting [12, 14, 17, 19, 21, 26, 27]. Some motivations and applications of this problem when restricted to the 2-sphere stretch from the classical *Thompson problem* of determining a configuration of N electrons on the surface of a unit sphere that minimises the electrostatic potential energy [16, 24], to search and rescue/exploration problems as well as problems related to extremal energy, crystallography and computational chemistry [17]. In the original offline version of the problem of distributing points

over some space, the number of points is predetermined and the goal is to distribute all points as uniformly as possible at the end of the process.

In contrast, the *online* optimisation problem requires that the points should be dynamically inserted one at a time on the surface of a sphere without knowing the total number of points in advance. Thus, the objective is to distribute the points as uniformly as possible at every instance of inserting a point. Note that in this case once a point has been placed *it cannot be later moved*. The points on the sphere correspond to unit quaternions and the group of rotations SO(3) [3, 18], which have a large number of engineering applications in the online setting (also known as "incremental generation") and plays a crucial role in applications ranging from robotics and aeronautics to computer graphics [27].

The online variant of distributing points in a given space has already been studied, e.g. for inserting integral points on a line [1] or on a grid [28], inserting real points over a unit cube [23] and also recently as a more complex version of inserting real points on the surface of a sphere [8, 27, 29]. A good strategy for online distribution of points on the plane has been found in [2, 23] based on the Voronoi insertion, where the gap ratio is proved to be at most 2. For insertion on a two-dimensional grid, algorithms with a maximal gap ratio $2\sqrt{2} \approx 2.828$ were shown in [28]. The same authors showed that the lower bound for the maximal gap ratio is 2.5 in this context. The other important direction was to solve the problem for the one-dimensional line and an insertion strategy with a uniformity of 2 has been found in [1]. An approach of using *generalised spiral points* was discussed in [16, 17], which performs well for minimizing extremal energy, but this approach is strictly offline (number of points N known in advance).

Recently the problem of *online distribution of points on the* 2-sphere has been proposed in [8] where a *two phase point insertion algorithm* with an overall upper bound of 5.99 was designed. The first phase uses a circumscribed dodecahedron to place the first twenty vertices, achieving a maximal gap ratio 2.618. After that, each of the twelve pentagonal faces can be recursively divided. This procedure is efficient and leads to a gap ratio of no more than 5.99. With more complex analysis, the bound was recently decreased to at most 3.69 in [29].

One may consider whether such two phase algorithms may perform well for this problem by either modifying the initial shape used in the first phase of the algorithm (such as using initial points derived from other Platonic solids) or else whether the recursive procedure used in phase two to tessellate each regular shape may be improved. We may readily identify an advantage to choosing a Platonic solid for which each face is a triangle (the tetrahedron, octahedron and icosahedron), since in this case at least two procedures for tessellating each triangle immediately spring to mind—namely to recursively place a new point at the centre of *each edge*, denoted *triangular dissection* (creating four subtriangles, see Fig. 2), or else the Delaunay tessellation, which is to place a new point at the *circumcentre of each triangle* (creating three new triangles, see Fig. 1).

It can be readily seen that the Delaunay tessellation of each spherical triangle rapidly gives a poor gap ratio, since points start to become dense around the centre of edges of the initial tessellation. The second recursive tessellation strategy (Fig. 2), was conjectured to give a poor ratio in [8]. This intuition seems reasonable, since as we
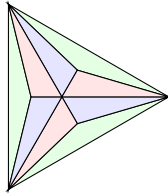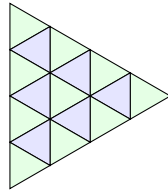
Fig. 1 Delauney triangulation applied twice

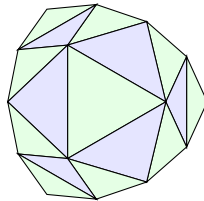**Fig. 2** Recursive triangle dissection (twice)

Fig. 3 Deformation of triangles in projection

recursively decompose each spherical triangle by this strategy the gap ratio increases as for such a triangle this decomposition deforms with each recursive step, as can be seen in Fig. 3. It can also be seen that the gap ratio at each level of the triangular dissection increases (see Lemma 4.4). Nevertheless, we show in this paper that as long as the initial tessellation (stage 1) does not create too 'large' spherical triangles (with high curvature), then the gap ratio of stage 2 has an upper limit, and performs much better than the tessellation of the regular dodecahedron proposed in [8] and [29].

In this paper, we provide a new algorithm and utilise a circumscribed regular icosahedron and the recursive triangular dissection procedure to reduce the bound of 3.69 derived in [29] to $\pi/\arccos(1/\sqrt{5}) \approx 2.8376$. Apart from a better upper bound, an advantage of our triangular tessellation procedure is its generalisability and more efficient tessellation as we only need to compute the spherical median between two locally introduced points at every step.

Another natural point insertion algorithm to consider is a greedy algorithm, where points are iteratively added to the centre of the largest empty circle. However, the decomposition of a 2-sphere according to the greedy approach leads to complex non-regular local structures and it soon becomes intractable to determine the next point to place [8, 29] (such points can in general even be difficult to describe in a computationally efficient way).

A preliminary version of this paper appeared in [4]. The present paper provides full details and diagrams for proofs, improves the lower bound of 1.618 to 1.726 in Theorem 5.5, provides some experimental results and shows in Sect. 5.1 a counterexample of a claimed lower bound of 1.78 from [29].

2 Notation

2.1 Spherical Trigonometry

Given a set P, we denote by 2^P the power set of P (the set of all subsets). Let $\mathcal{S}$ denote the 3-dimensional unit sphere (the 2-sphere). We will deal almost exclusively with unit spheres, since for our purposes the gap ratio (introduced formally later) is not affected by the spherical radius. Let $u_1, u_2, u_3 \in \mathbb{R}^3$ be three unit length vectors, then $T = \langle u_1, u_2, u_3 \rangle$ denotes the spherical triangle on $\mathcal{S}$ with vertices $u_1, u_2,$ and u_3. Given some set of points $\{u_1, u_2, u_3\} \cup \{v_j \mid 1 \leq j \leq k\}$, a spherical triangle $T = \langle u_1, u_2, u_3 \rangle$ is called *minimal* over that set of points if no v_j for $1 \leq j \leq k$ lies on the interior or boundary of T. As an example, in Fig. 5, triangle $\langle u_1, u_{113}, u_{112} \rangle$ is minimal, but $\langle u_1, u_{13}, u_{12} \rangle$ is not, since points u_{113} and u_{112} lie on the boundary of that triangle.

The edges of a spherical triangle are arcs of great circles. A great circle is the intersection of $\mathcal{S}$ with a central plane, i.e one which goes through the centre of $\mathcal{S}$. We denote the length of a path connecting two points u_1, u_2 on the unit sphere by $\zeta(u_1, u_2)$ (the spherical length).

Given a non-degenerate spherical triangle (i.e., one with positive area, defined later) with two edges e_1 and e_2 which intersect at a point P, then we say that the angle of P is the angle of P measured when projected to the plane tangent at P. We constrain all spherical triangles to have edge lengths strictly between 0 and π, which avoids issues with *antipodal triangles*. Two points on the unit sphere are called antipodal if the angle between them is π (i.e., they lie opposite to each other on the unit sphere) and an antipodal triangle contains two antipodal points. Several results in spherical trigonometry (and in this paper) are derived by projections of points/edges to planes tangent to a point on the sphere; in all such cases the projection is from the centre of the sphere.

The following results are all standard from spherical trigonometry, see [25] for proofs and further details. The length of an arc belonging to a great circle corresponds with the angle of the arc, see Fig. 4. Furthermore, given an arc between two points u_1 and u_2 on $\mathcal{S}$, the length of the line connecting u_1 and the projection of u_2 to the plane tangent to u_1 is given by $\tan(\zeta(u_1, u_2))$, see Fig. 4.

Lemma 2.1 (spherical laws of sines and cosines) *Given a spherical triangle with sides a, b, c and angles A, B, C opposite to side a, b, c resp., then:*

(i) $\cos c = \cos a \cos b + \sin a \sin b \cos C$;
(ii) $\cos C = -\cos A \cos B + \sin A \sin B \cos c$; *and*
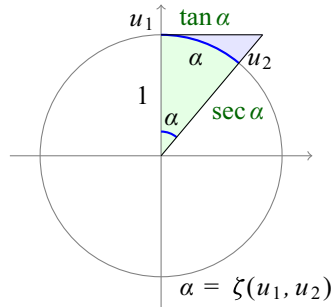(iii) $\sin a / \sin A = \sin b / \sin B$.

$$u_1 \quad \tan\alpha$$

$$\alpha \quad u_2$$

$$1$$

$$\alpha \quad \sec\alpha$$

$$\alpha = \zeta(u_1, u_2)$$

Fig. 4 Angular calculations in the plane intersecting the great circle containing (u_1, u_2)

The sum of angles within a spherical triangle is between π (as the area approaches zero) and 3π (as the triangle fills the whole sphere). The *spherical excess* of a triangle is the sum of its angles minus π radians.

Theorem 2.2 (Girard's theorem) *The area of a spherical triangle is equal to its spherical excess.*

2.2 Online Point Placing on the Unit Sphere

Our aim is to insert a sequence of 'uniformly distributed' points onto $\mathcal{S}$ in an online manner. After placing a point, it cannot be moved in the future. Let p_i be the i'th point thus inserted and let $S_i = \{p_1, p_2, \ldots, p_i\}$ be the configuration after inserting the i'th point. Teramoto et al. introduced the gap ratio [23], which defines a measure of uniformity for point samples and we use this metric (similarly to [8]).

Let $\rho_{\min}: 2^{\mathcal{S}} \to \mathbb{R}$ denote the minimal distance between a set of points S_i, defined by $\rho_{\min}(S_i) = \min_{p,q \in S_i, p \neq q} \zeta(p,q)$. Recall that notation $2^{\mathcal{S}}$ means the set of all points lying on the 2-sphere $\mathcal{S}$. Let $\rho_{\max}^{\mathcal{S}'}: 2^{\mathcal{S}} \to \mathbb{R}$ denote the maximal spherical diameter of the largest empty circle centred at some point of $\mathcal{S}' \subseteq \mathcal{S}$ not intersecting the given set of points S_i, defined by $\rho_{\max}^{\mathcal{S}'}(S_i) = \max_{p \in \mathcal{S}'} \min_{q \in S_i} 2 \cdot \zeta(p,q)$. We then define $\rho^{\mathcal{S}'}(S_i) = \rho_{\max}^{\mathcal{S}'}(S_i)/\rho_{\min}(S_i)$ to be the *gap ratio* of S_i over $\mathcal{S}'$. When $\mathcal{S}' = \mathcal{S}$ (i.e., when points can be placed anywhere on the sphere), we define that $\rho(S_i) = \rho^{\mathcal{S}}(S_i)$.

We denote an *equilateral* spherical triangle as one for which each side has the same length. By Lemma 2.1 (the spherical law of cosines), having three equal length edges implies that an equilateral spherical triangle has the same three angles. By Theorem 2.2 (Girard's theorem), each such angle is greater than $\pi/3$ (for an equilateral triangle of positive area). Let $\Delta \subseteq \mathcal{S}$ denote the set of all spherical triangles on the unit sphere.

Consider a spherical triangle $T \in \Delta$. We define a *triangular dissection* function $\sigma: \Delta \to 2^{\Delta}$ in the following way. If $T \in \Delta$ is defined by $T = \langle u_1, u_2, u_3 \rangle$, then $\sigma(T) = \{T_1, T_2, T_3, T_4\} \subset \Delta$, where $T_1 = \langle u_1, u_{12}, u_{13} \rangle$, $T_2 = \langle u_{12}, u_2, u_{23} \rangle$, $T_3 = \langle u_3, u_{13}, u_{23} \rangle$, and $T_4 = \langle u_{12}, u_{13}, u_{23} \rangle$, with u_{ij} being the midpoints (on the unit sphere) of the arc connecting u_i and u_j (see Fig. 5). Define $\sigma_E(T)$ as the set

of nine induced edges: $\{(u_1, u_{12}), (u_{12}, u_2), (u_2, u_{23}), (u_{23}, u_3), (u_3, u_{13}), (u_{13}, u_1),$ $(u_{13}, u_{23}), (u_{23}, u_{12}), (u_{12}, u_{13})\}$.

We extend the domain of σ to sets of spherical triangles: $\sigma(\{T_1, T_2, \ldots, T_k\}) = \{\sigma(T_1), \sigma(T_2), \ldots, \sigma(T_k)\}$; thus $\sigma: 2^\Delta \to 2^\Delta$. Given a spherical triangle $T \in \Delta$, we then define that $\sigma^1(T) = \sigma(T)$ and $\sigma^k(T) = \sigma(\sigma^{k-1}(T))$ for $k > 1$. For notational convenience, we also define that $\sigma^0(T) = T$ (the identity tessellation). We similarly extend $\sigma_E(T)$ to a set of triangles: $\sigma_E(\{T_1, T_2, \ldots, T_k\}) = \{\sigma_E(T_1), \sigma_E(T_2), \ldots, \sigma_E(T_k)\}$ and let $\sigma_E^k(T) = \sigma_E(\sigma^k(T_1), \sigma^k(T_2), \ldots, \sigma^k(T_k))$. See Fig. 5 for an example showing the tessellation of T to depth 2 (e.g. $\sigma^2(T)$) and the set of edges $\sigma_E^2(T)$.

Let $\mu: \Delta \to 2^S$ be a function which, for an input spherical triangle, returns the (unique) set of three points defining that triangle. For example, given a spherical triangle $T = \langle p_1, p_2, p_3 \rangle$, then $\mu(T) = \{p_1, p_2, p_3\}$. Clearly μ may be extended to sets of triangles by defining that $\mu(\{T_1, \ldots, T_k\}) = \{\mu(T_1), \ldots, \mu(T_k)\}$; thus $\mu: 2^\Delta \to 2^S$. When there is no danger of confusion, by abuse of notation, we sometimes write T rather than $\mu(T)$. This allows us to write $\rho(T)$ (or $\rho(\sigma^k(T))$) for example, as the gap ratio of the three points defining spherical triangle T (resp. the set of points in the k-fold triangular dissection $\sigma^k(T)$).

We will also require an ordering on the set of points generated by a tessellation $\sigma^k(T)$. Essentially, we wish to order the points as those of $\sigma^0(T) = T$ first (in any order), then those of $\sigma^1(T)$ in any order *but omitting the points of $\sigma^0(T) = T$*, then the points of $\sigma^2(T)$, omitting points in triangles of $\sigma^0(T)$ or $\sigma^1(T)$, etc. To capture this notion, we introduce a function $\tau: \Delta \times \mathbb{Z}^+ \to 2^S$ defined thus:

$$\tau(T, k) = \begin{cases} \mu(\sigma^k(T)) - \mu(\sigma^{k-1}(T)) & \text{if } k \geq 1, \\ \mu(T) & \text{if } k = 0. \end{cases}$$

As an example, in Fig. 5, $\tau(T, 0) = \{u_1, u_2, u_3\}$, $\tau(T, 1) = \{u_{12}, u_{13}, u_{23}\}$, and $\tau(T, 2) = \{u_{112}, u_{122}, u_{232}, u_{323}, u_{133}, u_{113}, u_{1323}, u_{1213}, u_{1223}\}$. By abuse of notation, we redefine $\sigma^k(T)$ so that $\sigma^k(T) = \tau(T, 0) \cup \tau(T, 1) \cup \ldots \cup \tau(T, k)$ is an
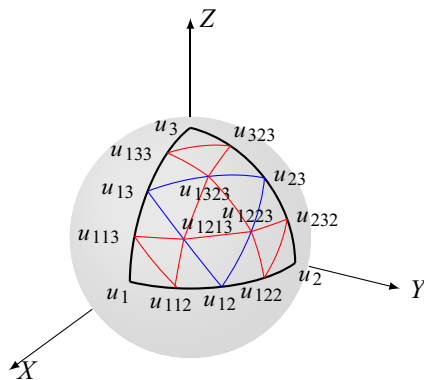

Fig. 5 σ tessellations

ordered set, ordered by points $\tau(T, 0)$ first and $\tau(T, k)$ last (points within any $\tau(T, j)$ for $1 \leq j \leq k$ are in any order).

3 Overview of Online Vertex Insertion Algorithm

Our algorithm is a two stage strategy. In stage one, we project the 12 vertices of the regular icosahedron onto the unit sphere. The first two points inserted should be opposite each other (antipodal points), but the remaining 10 points can be inserted in any order, giving a stage one gap ratio of $\pi/\arccos(1/\sqrt{5}) \approx 2.8376$.

In the second stage, we treat each of the 20 equilateral spherical triangles of the regular icosahedron in isolation. We show in Lemma 4.4 that the gap ratio for our tessellation is 'local' and depends only on the local configuration of vertices around a given point. This allows us to consider each triangle separately. During stage two, we use the fact that these twenty spherical triangles are equilateral and apply Lemma 7 to independently tessellate each triangle recursively in order to derive an upper bound of the gap ratio in stage two of $2(3 - \sqrt{5})/\arcsin\left(\sqrt{2 - 2/\sqrt{5}}/2\right) \approx 2.760$.

We note here that the radius of the sphere does not affect the gap ratio of the point insertion problem, and thus we assume a unit sphere throughout.

The algorithmic procedure to generate an infinite set of points is shown in Algorithm 1. To generate a set of k points $\{p_1, p_2, \ldots, p_k\}$, we choose the first k points generated by the algorithm.

Algorithm 1 Placing infinitely many points on the unit sphere using our recursive tessellation procedure on the regular icosahedron.

Stage one: Project 12 vertices of the icosahedron to the unit sphere:
Place two antipodal points on the unit sphere.
Place the remaining ten points in any order.
Arbitrarily label the 20 minimal spherical triangles $T = \{T_1, \ldots, T_{20}\}$.
Stage two: Recursively tessellate minimal triangles
Let $T' \leftarrow T$
while TRUE **do**
   for all minimal spherical triangles $R \in T$ **do**
      Let $T' \leftarrow (T' \cup \sigma(R)) - R$
   end for
   Let $T \leftarrow T'$
end while

---

4 Gap Ratio of Equilateral Spherical Triangles

We will require several lemmata regarding tessellations of spherical triangles. The following lemma is trivial from the spherical sine rule and Girard's theorem.

Lemma 4.1 *Let $T \in \Delta$ be an equilateral triangle. Then the central triangle in the tessellation $\sigma(T)$ is also equilateral.*

Proof Consider Fig. 5. The lemma claims that if $\langle u_1, u_2, u_3 \rangle$ is equilateral, then so is $\langle u_{12}, u_{13}, u_{23} \rangle$ (and therefore also $\langle u_{1213}, u_{1223}, u_{1323} \rangle$). As a consequence of the spherical cosine rule, an equilateral spherical triangle will have three equal interior angles, each of which is larger than $\pi/3$ (otherwise, by Girard's theorem, it has zero area). Since the edge lengths of T are identical, then the central triangle of $\sigma(T)$ also has equal length edges, again by the spherical cosine rule. □

It is worth emphasising in Lemma 4.1 that the other three triangles in the triangular dissection of an equilateral triangle are *not* equilateral, and have a strictly smaller area than the central triangle. This *deformation* of the recursive triangular dissection makes the analysis of the algorithm non-trivial. The following lemma equates the distance from the centroid of an equilateral spherical triangle to a vertex of that triangle. Note that the centroid and circumcentre coincide for an equilateral triangle and thus both terms can be used interchangeably.

Lemma 4.2 *Let* $T = \langle u_1, u_2, u_3 \rangle \in \Delta$ *be an equilateral triangle with circumcentre* u_c *and edge length* $\zeta(u_1, u_2) = \alpha$. *Then* $\zeta(u_1, u_c) = \zeta(u_2, u_c) = \zeta(u_3, u_c) = \arcsin(2\sin(\alpha/2\sqrt{3}))$.

Proof Consider Fig. 7. The circumcentre of T is, as for standard triangles, the unique point u_c of T from which the (spherical) distance satisfies $\zeta(u_c, u_1) = \zeta(u_c, u_2) = \zeta(u_c, u_3)$. Let then $x = \zeta(u_c, u_1)$. By the sine rule of spherical trigonometry:

$$\frac{\sin x}{\sin(\pi/2)} = \frac{\sin(\alpha/2)}{\sin(2\pi/6)},$$

and since $\sin(\pi/3) = \sqrt{3}/2$, then $x = \arcsin(2\sin(\alpha/2)/\sqrt{3})$. □

Given an equilateral spherical triangle T, we will also need to determine the maximal and minimal edge lengths in $\sigma_E^k(T)$ for $k \geq 1$, which we now show.

Lemma 4.3 *Let* $T = \langle u_1, u_2, u_3 \rangle \in \Delta$ *be an equilateral triangle such that* $\alpha = \zeta(u_1, u_2) \in (0, \pi/2]$ *and* $k \geq 1$. *Then the minimal length edge in* $\sigma_E^k(T)$ *is given by any edge lying on the boundary of* T. *The maximal length edge of* $\sigma_E^k(T)$ *is any of the edges of the central equilateral triangle of* $\sigma^k(T)$.

Proof Consider Fig. 5. The lemma states that in $\sigma^2(T)$ shown, the *shortest* length edge of $\sigma_E^2(T)$ is (u_1, u_{113}), or indeed any such edge on the boundary of triangle $\langle u_1, u_2, u_3 \rangle$. The lemma similarly states that the *longest* edge of $\sigma_E^2(T)$ is edge (u_{1213}, u_{1223}), or indeed any edge of the central equilateral triangle $\langle u_{1213}, u_{1223}, u_{1323} \rangle$.

Consider now Fig. 6 illustrating $T = \langle u_1, u_2, u_3 \rangle$. Point u_{12} (resp. u_{13}) is at the midpoint of spherical edge (u_1, u_2) (resp. (u_1, u_3)). Let $\alpha = \zeta(u_1, u_2) = \zeta(u_2, u_3) = \zeta(u_1, u_3)$ be the edge length. The intersection of spherical edges (u_2, u_{13}) and (u_1, u_3) forms a spherical right angle at u_{13}. We denote $y = \zeta(u_{13}, u_{12})$, thus y is the edge length of the central equilateral triangle of $\sigma(T)$ (and $\alpha/2 = \zeta(u_1, u_{13})$ is the edge length of the minimal length edge of one of the non-central triangles in $\sigma(T)$; note that this is the same for each such triangle).
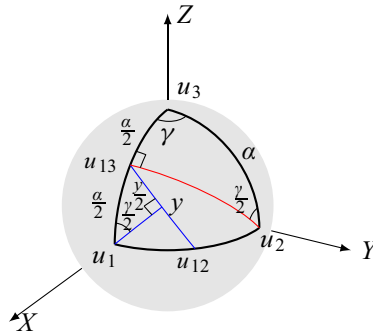
Fig. 6 Max and min lengths of σ tessellations of an equilateral triangle

By the spherical sine rule, $\sin(\gamma/2) = \sin(\alpha/2)/\sin\alpha$, which is illustrated by triangle $\langle u_2, u_{13}, u_3 \rangle$. Thus $\sin(\gamma/2) = \sec(\alpha/2)/2$. Here we used the (standard trigonometric) identity that $\sin(x/2)/\sin x = \sec(x/2)/2$. Further, one can see by the spherical sine rule that $\sin(y/2) = \sin(\alpha/2) \cdot \sin(\gamma/2) = \sin(\alpha/2)/(2\cos(\alpha/2)) = \tan(\alpha/2)/2$. This implies $\zeta(u_{13}, u_{12}) = y = 2\arcsin(\tan(\alpha/2)/2)$ which is larger than $\alpha/2$ for $\alpha \in (0, \pi/2]$. To prove this, let $f(\alpha) = 2\arcsin(\tan(\alpha/2)/2)$ then

$$\frac{\mathrm{d}f}{\mathrm{d}\alpha} = \frac{2}{\cos^2(\alpha/2)\sqrt{4 - \tan^2(\alpha/2)}}$$

as is not difficult to prove. Noting that if $\alpha \in (0, \pi/2]$, then $\cos^2(\alpha/2) \in [1/2, 1]$ and $\sqrt{4 - \tan^2(\alpha/2)} \in [2, \sqrt{3}]$, then $\mathrm{d}f/\mathrm{d}\alpha > 1/2 = \mathrm{d}(\alpha/2)/\mathrm{d}\alpha$ and thus since $f(\alpha) = 0 = \alpha/2$ when $\alpha = 0$, then $y > \alpha/2$ for $\alpha \in (0, \pi/2]$.

For any depth-k tessellation $\sigma^k(T)$, the maximal edge length of $\sigma_E^k(T)$ will thus be given by the length of the edges of the central equilateral triangle and the minimal length edges will be located on the boundary of T as required. □
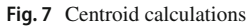
Given an equilateral spherical triangle $T = \langle u_1, u_2, u_3 \rangle$, we now consider the gap ratio implied by the restriction of points to those of T. The first part of this lemma shows that the gap ratio of a depth-k tessellation is lower than the gap ratio of a depth-$(k+1)$ tessellation (when restricted to points of T), and the second part shows that in the limit, the upper bound converges.

Lemma 4.4 *Let $T = \langle u_1, u_2, u_3 \rangle$ be an equilateral spherical triangle with spherical edge length α, then*

$$\rho^T(\mu(\sigma^k(T))) < \rho^T(\mu(\sigma^{k+1}(T))); \tag{i}$$

$$\lim_{k \to \infty} \rho^T(\mu(\sigma^k(T))) = \frac{4\sin(\alpha/2)}{\alpha\sqrt{3 - 4\sin^2(\alpha/2)}}. \tag{ii}$$

Proof Consider Fig. 7 and let $\alpha = \zeta(u_1, u_2) = \zeta(u_2, u_3) = \zeta(u_1, u_3)$ be the edge length of the equilateral triangle $T = \langle u_1, u_2, u_3 \rangle$. Calculate $\rho^T(\sigma^0(T)) = \rho^T(T)$.

Fig. 7 Centroid calculations

Note by abuse of notation that we write $\rho^T(T)$ rather than the more formal $\rho^T(\mu(T))$, as explained previously. Recall then that $\rho^T(T)$ denotes the gap ratio of point set $\mu(T)$ when the maximal gap ratio calculation is restricted to points of T.

We see that $\rho_{\min}(T) = \alpha$ since all edge lengths of T are identical. Clearly $\rho_{\max}^T(T) = 2x$; in other words the maximal spherical diameter of the largest empty circle centred inside T should be placed at the centroid (circumcenter) u_c of T. This follows since if the circle is centered at any other point of T, then it will be closer to at least one vertex of T and therefore $\rho_{\max}^T(T)$ would only decrease. Thus $\rho^T(\sigma^0(T)) = 2x/\alpha$.

By Lemma 4.1, triangle $\langle u_{12}, u_{23}, u_{13} \rangle$ in the decomposition $\sigma(T)$ is also equilateral. It is clear that $\beta > \alpha/2$ in Fig. 7 by the spherical sine rule, since $\gamma > \pi/3$ (by Girard's theorem). This implies that the largest empty circle will again be centred at the circumcentre of $\langle u_{12}, u_{23}, u_{13} \rangle$, which is the same as the circumcentre of $\langle u_1, u_2, u_3 \rangle$. Therefore, $\rho_{\min}(\sigma^1(T)) = \alpha/2$, $\rho_{\max}^T(\sigma^1(T)) = 2\beta$ and thus $\rho^T(\sigma^1(T)) = 4\beta/\alpha$. We now show that $2x/\alpha < 4\beta/\alpha$, which is true if $x < 2\beta$.

Let us consider the projection of equilateral spherical triangle $\langle u_1, u_2, u_3 \rangle$ from the centre of the unit sphere to a tangent plane at the point u_c. The point u_c is the circumcentre of spherical triangle $\langle u_1, u_2, u_3 \rangle$, as well its projection to the plane P, given by the planar triangle $\langle u_1', u_2', u_3' \rangle$.

The median of spherical triangle $\langle u_1, u_2, u_3 \rangle$ has length $x + \beta$. The range of x is from β to 2β. This follows from the fact that in the maximal equilateral spherical triangle case (i.e., when each angle is π and the triangle forms a half sphere) $\beta = x = \pi/2$ and when the area of the spherical triangle converges to zero, the median of the spherical triangle $\langle u_1, u_2, u_3 \rangle$ converges to the median of the triangle projection $\langle u_1', u_2', u_3' \rangle$, and x converges to 2β as the centroid/circumcentre of an equilateral Euclidean triangle divides each median in the ratio $2:1$.

We thus see that the gap ratio of the (six) points of $\sigma^1(T)$ is greater than the gap ratio of the (three) points of $\sigma^0(T)$, when restricted to points of T. Since the maximal ratio is calculated by using a circle centred at the circumcentre of the triangle T, this argument applies recursively and for each tessellation $\sigma^k(T)$, the maximal ratio is given by twice the distance of the circumcentre to the vertices of the central equilateral triangle of the tesselation by Lemma 4.3, and therefore the gap ratio increases at each

depth of the tessellation, which proves statement one of the lemma. We will now determine $\lim_{k\to\infty}\rho^T(\sigma^k(T))$ to prove the second statement.

We may observe that $\rho_{\min}(\sigma^k(T)) = \alpha/2^k$, since the outer edges of triangle T (with length α) are subdivided into two k times under $\sigma^k(T)$ and all interior edges have greater length. As explained above, the maximal diameter circle which may be placed on a point of T which does not intersect points of $\sigma^k(T)$ will be centred at the circumcentre u_c of T and have a diameter twice the distance from u_c to a vertex of that triangle.

Construct a plane P_{u_c} tangent to the point u_c (the circumcentre of T). In Fig. 7, note that $x = \zeta(u_1, u_c) = \arcsin(2\sin(\alpha/2)/\sqrt{3})$ by Lemma 4.2. The distance[1] from the circumcentre point to a vertex projected by points u_1, u_2, or u_3 is given by $\tan x$ (see Fig. 4 and Sect. 2.1), thus the edges of the projection of triangle T have length $y = \sqrt{3}\tan x$ since the projection of an equilateral triangle about its circumcentre from the origin to P_{u_c} is equilateral, with the same circumcentre (and the distance from the centroid/circumcentre of an equilateral Euclidean triangle to any vertex is of course given by $e/\sqrt{3}$, where e is the edge length of the triangle). The central tessellated triangle thus has edges whose length starts to approximate $(\sqrt{3}\tan x)/2^k$ in the limit, since as $k \to \infty$, then this triangle lies on the plane tangent at u_c (i.e., the difference between the edge length of the spherical triangle and its projection decreases to zero). This implies that the maximal spherical diameter of the largest empty circle centred at u_c is the distance from u_c to one of these vertices, which approaches $2\tan x/2^k$ in the limit as $k \to \infty$. Therefore,

$$\lim_{k\to\infty}\rho^T(\sigma^k(T)) = \lim_{k\to\infty}\frac{\rho_{\max}^T(\sigma^k(T))}{\rho_{\min}(\sigma^k(T))} = \lim_{k\to\infty}\frac{(2\tan x)/2^k}{\alpha/2^k}$$

$$= \frac{2\tan(\arcsin(2\sin(\alpha/2)/\sqrt{3}))}{\alpha} \tag{1}$$

$$= \frac{4\sin(\alpha/2)}{\alpha\sqrt{3-4\sin^2(\alpha/2)}}. \tag{2}$$

Moving from (1) to (2), we used the identity $\tan(\arcsin x) = x/\sqrt{1-x^2}$. $\qquad\square$

5 Regular Icosahedral Tessellation

As explained in Sect. 3 and Algorithm 1, our algorithm consists of two stages. Using the lemmata of the previous section, we are now ready to show that the stage one gap ratio is no more than $\pi/\arccos(1/\sqrt{5}) \approx 2.8376$ and the second stage gap ratio is no more than

---

[1] Note that here we refer to the Euclidean distance between the points, rather than the spherical distance, since the projected points are not on the sphere

$$\frac{2(3 - \sqrt{5})}{\arcsin\left(\sqrt{2 - 2/\sqrt{5}}/2\right)} \approx 2.760.$$

Lemma 5.1 *The gap ratio of stage one is no more than* $\pi/\arccos(1/\sqrt{5}) \approx 2.8376$.

Proof The points of a regular icosahedron can be defined by taking circular permutations of $(0, \pm 1, \pm\phi)$, where $\phi = (1 + \sqrt{5})/2$ is the golden ratio. Let V' be the set of the twelve such vertices. Normalising each element of V' gives a set V. Note that the area of each spherical triangle is given by $\pi/5$ since we have a unit sphere and twenty identical spherical triangles forming a tessellation. By Girard's theorem (Theorem 2.2), this implies that $3\gamma - \pi = \pi/5$, where γ is the interior angle of the equilateral triangle and thus $\gamma = 2\pi/5$. By the second spherical law of cosines (Lemma 2.1), this implies that the spherical distance between adjacent vertices, α, is thus given by

$$\cos\alpha = \frac{\cos(2\pi/5) + \cos^2(2\pi/5)}{\sin^2(2\pi/5)} = \frac{(\sqrt{5} - 1)/4 + 3/8 + \sqrt{5}/8}{5/8 + \sqrt{5}/8}$$
$$= \frac{(1 + \sqrt{5})/8}{(5 + \sqrt{5})/8} = \frac{1}{\sqrt{5}}$$

and therefore $\alpha \approx 1.1071$. The first two points are placed opposite to other, for example $u_1 \approx (0, -0.5257, 0.8507)$ and $u_2 \approx (0, 0.5257, -0.8507)$. At this stage, the gap ratio is 1, since the largest circle may be placed on the equator (with u_1 and u_2 at the poles) with a diameter of π, whereas the spherical distance between u_1 and u_2 is π. The remaining ten vertices of the normalised regular icosahedron are placed in any order. The minimal distance between them is given by α above, and thus the gap ratio during stage one is no more than $\pi/\arccos(1/\sqrt{5}) \approx 2.8376$, as required. □

As explained in Sect. 3 and Algorithm 1, we start with the twenty equilateral spherical triangles produced in stage one, denoted the depth-0 tessellation of $\mathcal{S}$. We apply σ to each such triangle to generate $20 * 4 = 80$ smaller triangles (note that not all such triangles are equilateral, in fact only eight triangles at each depth tessellation are equilateral). At this stage we have the depth-1 tessellation of $\mathcal{S}$. We recursively apply σ to each spherical triangle at depth-k to generate the depth-$(k+1)$ tessellation, which contains $20 * 4^{k+1}$ spherical triangles.

Lemma 5.2 *The gap ratio of stage two is no more than* $(12 - 4\sqrt{5})/\arccos(1/\sqrt{5}) \approx 2.760$.

Proof At the start of stage two, we have 20 equilateral spherical triangles, $T_1, \ldots, T_{20}$ which are identical (up to rotation). Note that moving from depth-k tessellation to depth-$(k + 1)$, each edge of $\sigma_E^k(T_i)$ will be split at its midpoint, therefore applying σ to any spherical triangle will only 'locally' change the gap ratio of at most two adjacent triangles. Thus the order in which σ is applied to each triangle at depth k is irrelevant.

Assume that we have a (complete) depth-k tessellation with $20 * 4^k$ triangles. Lemma 4.4 tell us that the gap ratio increases from the depth-k to the depth-$(k + 1)$ tessellations for all $k \geq 0$ and in the limit, the gap ratio of the depth-k tessellation of each T_i is given by

$$\lim_{k \to \infty} \rho^T (\sigma^k (T_i)) = \frac{4 \sin (\alpha/2)}{\alpha \sqrt{3 - 4 \sin^2 (\alpha/2)}}, \tag{3}$$

where α is the length of the edges of T_i (i.e., the length of those triangles produced by stage 1 via the icosahedron). When we start to tessellate the depth-k spherical triangles, until we have a complete depth-$(k+1)$ tessellation, applying σ to each of the triangles may decrease the minimal gap ratio at most by a factor up to 2 overall (since we split each edge at its midpoint). The maximal gap ratio cannot increase, but decreases upon completing the depth-$(k+1)$ tessellation. Therefore, we multiply the right hand side of (3) by 2 to obtain an upper bound of the gap ratio for the entire sequence, not only when some depth-k tessellation is complete. We now compute the right hand side of (3), after multiplying by 2, by substituting $\alpha = \arccos (1/\sqrt{5}) \approx 1.1071$. This is laborious, but by noting that $\sin (\alpha/2) = \sqrt{(5 - \sqrt{5})/10}$ and $\sin^2 (\alpha/2) = (5 - \sqrt{5})/10$, then

$$\frac{8 \sin (\alpha/2)}{\alpha \sqrt{3 - 4 \sin^2 (\alpha/2)}} = \frac{8 \sqrt{(5 - \sqrt{5})/10}}{\arccos (1/\sqrt{5}) \sqrt{1 + 2/\sqrt{5}}} = \frac{12 - 4\sqrt{5}}{\arccos (1/\sqrt{5})} \approx 2.760.$$

Therefore, the gap ratio during stage two is upper bounded by 2.76. □

Theorem 5.3 *The gap ratio of the icosahedral triangular dissection is equal to* $\pi/\arccos (1/\sqrt{5}) \approx 2.8376$.

Proof This is a corollary of Lemmas 5.1 and 5.2. Stage one of the algorithm has a larger gap ratio than stage two in this case. □

We can now prove the first non-trivial lower bound when we have only two or three points on the sphere in this online version of the problem.

Theorem 5.4 *The gap ratio for the online problem of placing the first three points on the sphere cannot be less than* $(1 + \sqrt{5})/2 \approx 1.6180$.

Proof Let us first estimate the ratio with only two points when one point is located at the north pole of the 2-sphere and the other is shifted by a distance x from the south pole. The gap ratio in this case is $(\pi + x)/(\pi - x)$, which increases from 1 to ∞ when $x \geq 0$.

Let us now consider the case with three points. If we place the third point on the plane P defined by the centre of the sphere and the other two points, then the gap ratio will be $\pi/((\pi + x)/2) = 2\pi/(\pi + x)$ as in this case the maximal diameter of an empty circle is π regardless of the position of the third point on P. Note that the centre of the largest circle not intersecting points p_1, p_2, p_3 will be orthogonal to
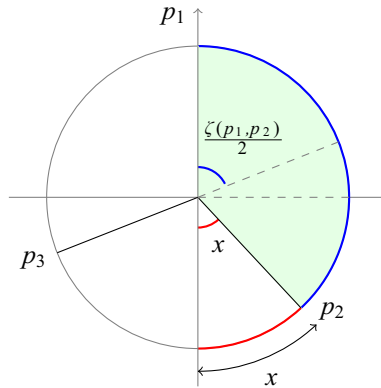
Fig. 8 Optimal placement of first three points to minimise gap ratio

these three points (giving the diameter of the largest empty circle as at least π) and the minimal distance between two points can be maximised by positioning the third point at the largest distance from the initial two points so that the closest two points have a distance of $(\pi + x)/2$.

If the third point is not on the plane P then the ratio will be equal to some value a/b that is larger than $2\pi/(\pi + x)$. This follows from the fact that the value a which is the maximal gap would be greater than π and the minimal gap b would be less than $(\pi + x)/2$. So the minimal gap ratio that can be achieved for the three points will be represented by the expression $2\pi/(\pi + x)$. See Fig. 8.

By solving the equation where the left hand side represents the gap ratio in the case of three points (a decreasing function) and the right hand side representing the case with two points (an increasing function), we find a positive value of the one unknown x: $2\pi/(\pi + x) = (\pi + x)/(\pi - x)$. The only positive value x satisfying the above equation has the value $\pi(\sqrt{5} - 2)$ and the gap ratio for this value x is equal to $(1 + \sqrt{5})/2$. □

We now show that by considering the first four points, we can do slightly better in lower bounding the minimal gap ratio.

Theorem 5.5 *The gap ratio for the online problem of placing four or more points on the sphere is greater than* 1.726.

Proof Consider Fig. 10. As in the previous proof, we begin by placing the first point u_1 at the north pole and the second point u_2 at some distance x from the south pole on the $z = 0$ plane, without loss of generality. We use an ansatz to estimate that for four points, the gap ratio cannot be less than 1.726. In order that the gap ratio for the first two points is not greater than 1.726, we have that

$$\frac{\pi + x}{\pi - x} \le 1.726 \quad \Rightarrow \quad x \le \frac{0.726}{2.726}.$$

To minimise the gap ratio after placing the third and fourth points, u_3 should be placed on the great circle A lying equidistantly between u_1 and u_2, shown in Fig. 10. To see
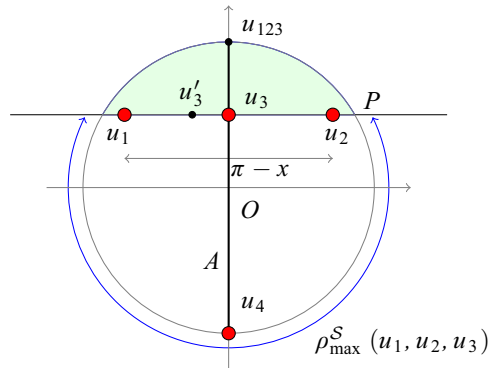
Fig. 9 Plane P intersecting u_1, u_2, u_3 and optimal position for u_4. A is the great circle equator of u_1, u_2

this, assume that u_3' is not placed on A and consider the plane P which is determined by points u_1, u_2, and u_3 as shown in Fig. 9. Let u_3 be the point lying on the intersection between P and A in the same hemisphere as u_3'. The centre of the largest empty circle of S after placing u_1, u_2, and u_3' is the optimal position for point u_4 since placing u_4 at this point minimises the largest remaining empty circle and maximises the distance to the closest existing point (shown by $\rho_{\max}^{\mathcal{S}}(u_1, u_2, u_3)$ in Fig. 9). The centre of the largest empty circle after placing u_1, u_2, and u_3' is either at the antipodal point of the circumcentre of $\langle u_1, u_2, u_3 \rangle$ if u_3 lies outside the circle on S containing u_1, u_2, or else at the antipodal point of the midpoint of u_1, u_2 if u_3 lies within this circle (i.e., if u_3 is in the top green segment of Fig. 9 where the plane P is then defined as intersecting u_1, u_2 and parallel to the tangent plane of the midpoint of u_1 and u_2). In the second case, the position of u_3 has no impact on the maximal empty circle and thus we may place u_3' on the arc A without loss of generality. We therefore consider the first case when u_3' is not within the circle containing u_1, u_2 and denote by u_4 the position of the centre of the largest empty circle, at the antipodal point of the circumcentre of u_1, u_2, u_3 as is shown in Fig. 9. Note that this point is identical for either $\langle u_1, u_2, u_3' \rangle$ or $\langle u_1, u_2, u_3 \rangle$ since u_3' and u_3 lie on the same plane P and thus share the same circumcircle. The spherical distance from u_3 to the closest of u_1 or u_2 is clearly smaller than the distance of u_3' to either of u_1 or u_2 by the definition of A (again shown in Fig. 9) and thus the gap ratio of sequence u_1, u_2, u_3, u_4 is no larger than the gap ratio of u_1, u_2, u_3', u_4. We therefore assume that u_3 lies on arc A and u_4 is placed at the antipodal point of the centre of the circumcircle of $\langle u_1, u_2, u_3 \rangle$. □

Let us thus assume that $x = 0.726/2.726$ and fix u_1 and u_2. Consider again Fig. 10. As z (the distance along the great arc A) increases from 0 (when u_3 is at the midpoint of u_1 and u_2) to π (at the antipodal point of the midpoint of u_1 and u_2), the gap ratio of $\{u_1, u_2, u_3\}$ decreases, since the minimal distance between points only increases and the size of the maximal empty circle (located either at the antipodal point of the centre of the circumcircle of $\langle u_1, u_2, u_3 \rangle$ or else at the antipodal point of the midpoint of u_1, u_2) monotonically decreases.
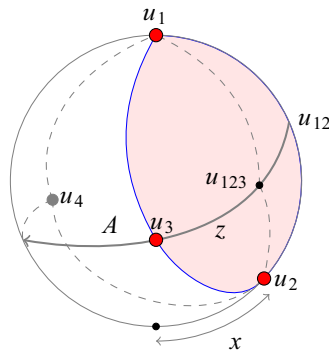
Fig. 10 Optimal positions of u_3 and u_4 for fixed u_1 and u_2. Point u_{123} is the circumcentre of u_1, u_2, u_3 and u_{12} is the midpoint of u_1 and u_2
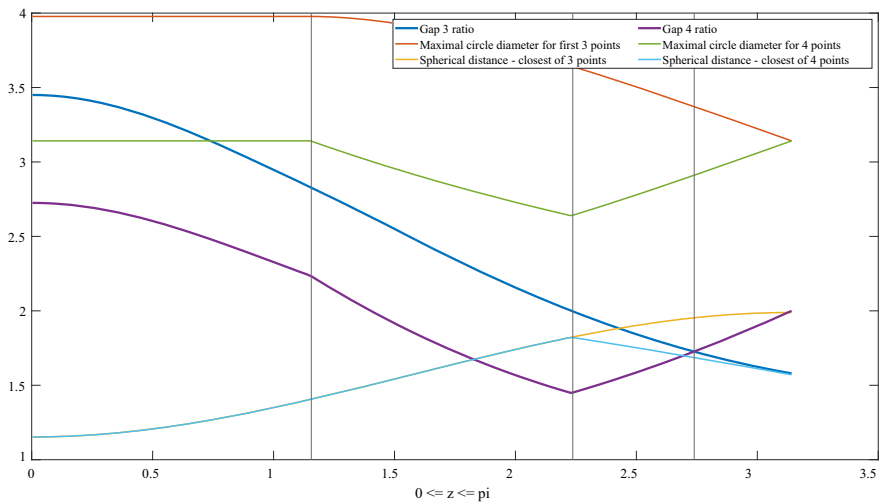

Fig. 11 Gap-3 and gap-4 ratios for various z when $x = 0.726\pi/2.726$

Let us denote by the *gap*-4 ratio the gap ratio of the four points u_1, u_2, u_3, u_4 ignoring the gap ratios of the subsequences u_1, u_2 and u_1, u_2, u_3 (similarly for the gap-3 ratio, which ignores the gap ratio of u_1, u_2). The gap-4 ratio of u_1, u_2, u_3, u_4 for z in the range $[0, \pi]$ can be split into four segments as can be seen in Fig. 11. We will show that the optimal gap ratio occurs at the unique point where the gap-3 and gap-4 ratios cross.

Since we have shown that the gap-3 ratio is monotonically decreasing, decreasing z from the intersection point of gap-3 and gap-4 ratios only only increases the overall gap ratio (which is the maximum of the two). At the intersection point, we have the

following four points:

$$u_1 = \begin{pmatrix} 0 \\ 1 \\ 0 \end{pmatrix}, \quad u_2 = \begin{pmatrix} 0.742 \\ -0.670 \\ 0 \end{pmatrix}, \quad u_3 = \begin{pmatrix} -0.841 \\ -0.374 \\ 0.392 \end{pmatrix}, \quad u_4 = \begin{pmatrix} -0.259 \\ -0.115 \\ -0.959 \end{pmatrix}.$$

As z increases from this intersection point, the gap-4 ratio increases which we now prove. Consider again Fig. 9. As z increases, the plane P moves downwards towards the origin since the circumcircle of $\langle u_1, u_2, u_3 \rangle$ has an increasing diameter. Once $\rho^{\mathcal{S}}_{\max}(u_1, u_2, u_3) = 2\zeta(u_4, u_1) < 2\pi/3$, then the largest empty circle of $\{u_1, u_2, u_3, u_4\}$ is located at the antipodal point of u_4, i.e., the centre of the circumcircle of $\langle u_1, u_2, u_3 \rangle$, which we denote u_{123} in Fig. 9. Note that by the definition of circumcircle $\zeta(u_1, u_{123}) = \zeta(u_2, u_{123}) = \zeta(u_3, u_{123})$ and note also that $\zeta(u_1, u_{123}) + \zeta(u_1, u_4) = \pi$, as is clear from the Fig. 9.

The closest two points of $\{u_1, u_2, u_3\}$ is given by $\zeta(u_1, u_3) = \zeta(u_2, u_3)$. This follows since $\zeta(u_1, u_2) > 2\pi/3$ and thus for any $z \in [0, \pi]$ then $\zeta(u_1, u_3) = \zeta(u_2, u_3) < \zeta(u_1, u_2)$. Since u_4 is at the antipodal point of the circumcentre of $\langle u_1, u_2, u_3 \rangle$, then $\zeta(u_1, u_4) = \zeta(u_2, u_4) = \zeta(u_3, u_4)$. Thus, once $\zeta(u_4, u_1) < \zeta(u_3, u_1)$ then we know that

$$\zeta(u_4, u_1) = \zeta(u_4, u_2) = \zeta(u_4, u_2) < \zeta(u_1, u_3) = \zeta(u_2, u_3) < \zeta(u_1, u_2)$$

For u_1, u_2, u_3, u_4 given above, the closest two points are therefore given by $\zeta(u_1, u_4) = 1.686 < 2\pi/3$ since $\zeta(u_1, u_4) < \zeta(u_1, u_3) = 1.954 < \zeta(u_1, u_2) = 2.305$. The largest empty circle of $\{u_1, u_2, u_3, u_4\}$ is thus given by w_{123}. Finally, consulting Fig. 9 once more, since increasing z moves the plane P towards the origin, we decrease $\zeta(u_1, u_4)$ and increase the maximum empty circle diameter given by $\zeta(u_1, u_{123})$ and thus the gap-4 ratio necessarily increases. Therefore, the optimal gap ratio for fixed u_1 and u_2 and for $z \in [0, \pi]$ is at this intersection point, corresponding to points u_1, u_2, u_3, u_4 given above.

The gap ratios of $\{u_1, u_2, u_3, u_4\}$ can be calculated as follows: $\rho(u_1, u_2) = 1.726$, $\rho(u_1, u_2, u_3) = 1.7261$ and $\rho(u_1, u_2, u_3, u_4) = 1.7261$. Note that u_3 is placed on the arc A equidistant from u_1 and u_2 (since $\zeta(u_1, u_3) = \zeta(u_2, u_3) = 1.9538$) as required, and that u_4 is in the opposite hemisphere from u_3 with $\zeta(u_1, u_4) = \zeta(u_2, u_4) = \zeta(u_3, u_4) = 1.686$. Now, since the gap ratios of points $\{u_1, u_2, u_3\}$ and $\{u_1, u_2, u_3, u_4\}$ are equal to 1.7261, and as pointed out earlier, as z increases the gap ratio of $\{u_1, u_2, u_3, u_4\}$ increases, and as z decreases the gap ratio of $\{u_1, u_2, u_3\}$ increases, then for fixed u_1 and u_2, these points u_3 and u_4 are optimal.

It remains to reason about out choice of x (the spherical distance from u_1 to u_2). We know that $x \leq 0.726\pi/2.726$, otherwise the gap ratio of the first two points is already above the bound of 1.726 and we have now analysed the case where we have equality.

Consider Fig. 10. For any $x' \in [0, 0.726\pi/2.726]$, there exists some choice of z_2 such that $\zeta(u_3, u_1) = \zeta(u_3, u_4)$. This is clear from the intermediate value theorem. The centre of the largest empty circle for u_1, u_2, u_3 is at the antipodal point of the

circumcentre of u_1, u_2, u_3, denoted u_4. Since $\zeta(u_3, u_1) = \zeta(u_3, u_4)$, then

$$\zeta(u_2, u_3) = \zeta(u_1, u_3) = \zeta(u_3, u_4) = \zeta(u_1, u_4) = \zeta(u_2, u_4).$$

The first equality is due to u_3 being placed on arc A and the latter two equalities are due to u_4 being at the antipodal point of the circumcentre of u_1, u_2, u_3. Since $\zeta(u_3, u_4) = \zeta(u_1, u_3)$, then the gap ratio is given by $2\zeta(u_3, u_4)/\zeta(u_3, u_1) = 2$. The numerator is derived since u_4 is the centre of the largest empty circle for u_1, u_2, u_3 and the denominator denotes the closest two points. For larger values of z, the maximal empty circle diameter of the first three points decreases and the centre of the largest empty circle is located at the circumcentre of the first three points (u_{123} in Figs. 9 and 10). For any choice of $x \leq 0.726\pi/2.726$, if the gap ratio is to be less than 2 we may thus assume that z is chosen so that any increase in z increases $\zeta(u_1, u_3)$ and the centre of the largest empty circle is located at u_{123}, the circumcentre of $\langle u_1, u_2, u_3 \rangle$.

Consider Fig. 9 and assume the figure corresponds to the optimal choice of z for $x = 0.726\pi/2.726$. As x decreases, the distance between points u_1 and u_2 increases and the distance from point u_3 to u_1 and u_2, for the same z value, will decrease. In order that the gap-3 ratio of the first three points does not increase, the plane P needs to move towards the origin, since the distance $\zeta(u_1, u_3)$ has decreased as x decreased. Now consider the gap-4 ratio. Since P has moved towards the origin, the minimal distance between points can only decrease. The centre of the maximal empty circle after placing u_1, u_2, u_3, u_4 is located at the circumcentre u_{123} of $\langle u_1, u_2, u_3 \rangle$ and the diameter of this circumcircle increases as P moves towards the origin. This implies that as x decreases the gap ratio must increase and thus $x = 0.726\pi/2.726$ is optimal.

5.1 Counterexample of Lower Bound 1.78

[29, Thm. 2] claims a lower bound of 1.78 for the gap ratio of online insertion of points onto the 2-sphere. The result is based on [29, Lem. 1] which derives the lower bound by considering three points and claiming that 1.78 is optimal. This contradicts the (constructive) proof in the present paper of Lemma 5.4 which shows how to generate three points whose gap ratio is $(1 + \sqrt{5})/2$ exactly.[2]

The issue with Theorem 2 of [29] appears to be in the final line of reasoning of the proof. The authors derive that $0.719\pi \leq \beta \leq 0.764\pi$, where $\beta = \zeta(u_1, u_2)$ and calculate that $\gamma = \pi\beta/(2\pi - \beta)$ with $\gamma = \zeta(u_2, u_3)$. It is then claimed "...the gap ratio is a decreasing function w.r.t. β" which appears incorrect. In order that the gap-2 and gap-3 ratios are identical, the authors derive that $\gamma = \pi\beta/(2\pi - \beta)$. Now, $\beta = 0.719\pi$ gives $\gamma = 1.763$ and thus a gap ratio of 1.78. However this is not optimal given that u_1, u_2, u_3, O lie on the same plane and thus $\zeta(u_1, u_3) = 2\pi - \beta - \gamma = 2.261 > \zeta(u_2, u_3) = \gamma$. When placing u_3 on the plane containing O, u_1, u_2, the optimal position lies equidistant to u_1 and u_2, since that maximises the minimum distance between points, with the maximal empty circle unaffected (and of

---

[2] Indeed, the three points can be calculated as $u_1 = (0, 1, 0)$, $u_2 = (-0.725, -0.688, 0)$, and $u_3 = (-0.395, -0.919, 0)$, where $\zeta(u_1, u_2) = 2.3299$ and $\zeta(u_2, u_3) = \zeta(u_1, u_3) = 1.9766$.

Table 1 The gap ratio of the depth-k tessellation of the regular icosahedron when isolated to an equilateral spherical triangle T

Depth of Tessellation	$\rho^T_{\min}(\sigma^k(T))$	$\rho^T_{\max}(\sigma^k(T))$	$\rho^T(\sigma^k(T))$	$2 \cdot \rho^T(\sigma^k(T))$
0	1.1071	1.3047	1.1784	2.3568
1	0.5536	0.7297	1.3182	2.6364
2	0.2768	0.3774	1.3636	2.7272
$\vdots$	$\vdots$	$\vdots$	$\vdots$	$\vdots$
7	0.0086	0.0119	1.3800	2.7600

Table 2 The gap ratio of stage one and two of various regular Platonic solids

	Tetrahedron	Octahedron	Dodecahedron	Icosahedron
Stage 1	2.289	2.0	2.618	*2.8376*
Stage 2	*5.921*	*3.601*	*5.995*	2.760

Italic elements show which value defines the overall gap ratio in each case

diameter π). Placing u_3 at this position would thus decrease the claimed lower bound of the gap ratio for three points.

6 Conclusion

In order to illustrate the rate of convergence of the gap ratio for various depths of tessellations starting from a single equilateral triangle of the regular icosahedron T, we wrote a program to perform recursive triangular dissection and to measure the minimum and maximum ratios. The results are shown in Table 1.

The table shows that starting from T, the gap ratio of the complete depth-k tessellation of T quickly approaches 1.38. The next point inserted after reaching a complete depth-k tessellation (with $12 * 4^k$ minimal triangles), requires us to split one of the edges in half according to Algorithm 1. This decreases the minimum gap ratio by a factor of $1/2$ which increases the gap ratio by a factor of 2. Therefore $2 \cdot \rho^T(\sigma^k(T))$ shows the maximal gap ratio at any point, not only restricted to complete depth-k tessellations.

To evaluate the most appropriate initial shape for our algorithm, we derived (both theoretically and with a computational simulation) the gap ratios of the stage 1 and stage 2 tessellations of various Platonic solids, shown in Table 2. The results for the dodecahedron are from [8] using a different tessellation (the dodecahedron has non-triangular faces). An illustration of the first stage of the octahedral and icosahedral spherical tessellations is shown in Figs. 12 and 13 respectively.

The results match our intuition, that a finer grained initial tessellation such as that from an icosahedron performs much better in stage 2 than a more coarse grained initial tessellation such as that from a tetrahedron. This is illustrated by Fig. 3 which shows that for a large initial equilateral spherical triangle, the recursive triangu-
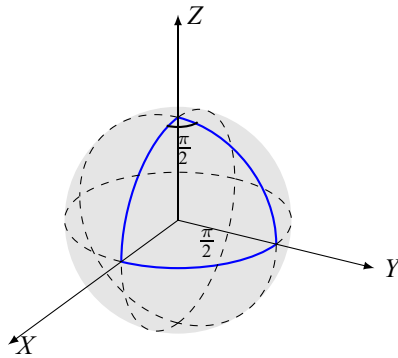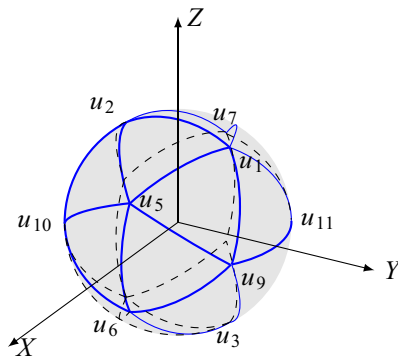
Fig. 12 Octahedral spherical tessellation

Fig. 13 Icosahedral spherical tessellation

lar dissection procedure deforms the four triangle by a larger margin. The regular icosahedron thus has the essential criteria that we require; it has a low stage 1 and stage 2 gap ratio, and it is a regular tessellation into equilateral spherical triangles. It would be interesting to consider modifications of the stage 2 procedure which may allow the octahedron to be utilised, given its low stage 1 gap ratio. This may require some a modification of Lemma 4.4 which works also with non-equilateral spherical triangles.

It would also be beneficial to tighten the lower bound. In Theorem 5.4 we derive the lower bound of 1.618 by considering the first three points and in Theorem 5.5 we consider the first four points to derive a lower bound of 1.726. Our proof technique shows that considering the first three or four points gives one or two degrees of freedom respectively. Even with two degrees of freedom the reasoning becomes significantly more challenging and therefore a different approach may be necessary in order to derive a reasonable increase in the lower bound.

A further avenue for future research would be to study relations to spherical t-designs. We thank one of the reviewers for pointing out this possible direction and we plan to look into this in a future paper.

References

1. Asano, T.: Online uniformity of integer points on a line. Inf. Process. Lett. **109**(1), 57–60 (2008)
2. Asano, T., Teramoto, S.: On-line uniformity of points. In: 8th Hellenic-European Conference on Computer Mathematics and Its Applications (Athens 2007), pp. 21–22 (2007)
3. Bell, P, Potapov, I.: Reachability problems in quaternion matrix and rotation semigroups. Inf. Comput. **206**(11), 1353–1361 (2008)
4. Bell, P.C., Potapov, I.: Towards uniform online spherical tessellations. In: 15th Conference on Computability in Europe (Durham 2019). Lecture Notes in Computer Science, vol. 11558, pp. 120–131. Springer, Cham (2019)
5. Bondarenko, A.V., Hardin, D.P., Saff, E.B.: Mesh ratios for best-packing and limits of minimal energy configurations. Acta Math. Hungar. **142**(1), 118–131 (2014)
6. Brauchart, J.S., Grabner, P.J.: Distributing many points on spheres: minimal energy and designs. J. Complex. **31**(3), 293–326 (2015)
7. Chazelle, B.: The Discrepancy Method. Randomness and Complexity. Cambridge University Press, Cambridge (2000)
8. Chen, Ch., Lau, F.C.M., Poon, Sh.-H., Zhang, Y., Zhou, R.: Online inserting points uniformly on the sphere. In: WALCOM: Algorithms and Computation (Hsinchu 2017). Lecture Notes in Computer Science, vol. 10167, pp. 243–253. Springer, Cham (2017)
9. Curl, R.F., Smalley, R.E.: Fullerenes. Sci. Am. **265**(4), 54–63 (1991)
10. Etayo, U.: Spherical cap discrepancy of the diamond ensemble. Discrete Comput. Geom. **66**(4), 1218–1238 (2021)
11. Guruswami, V., Micciancio, D., Regev, O.: The complexity of the covering radius problem. Comput. Complex. **14**(2), 90–121 (2005)
12. Hardin, D.P., Saff, E.B.: Discretizing manifolds via minimum energy points. Not. Am. Math. Soc. **51**(10), 1186–1194 (2004)
13. Koay, Ch.G.: Distributing points uniformly on the unit sphere under a mirror reflection symmetry constraint. J. Comput. Sci. **5**(5), 696–700 (2014)
14. Lubotzky, A., Phillips, R., Sarnak, P.: Hecke operators and distributing points on the sphere. I. Commun. Pure Appl. Math. **39**(suppl.), S149–S186 (1986)
15. Matoušek, J.: Geometric Discrepancy. An Illustrated Guide. Algorithms and Combinatorics, vol. 18. Springer, Berlin (1999)
16. Rakhmanov, E.A., Saff, E.B., Zhou, Y.M.: Minimal discrete energy on the sphere. Math. Res. Lett. **1**(6), 647–662 (1994)
17. Saff, E.B., Kuijlaars, A.B.J.: Distributing many points on a sphere. Math. Intell. **19**(1), 5–11 (1997)
18. Shoemake, K.: Uniform random rotations. In: Graphics Gems III, pp. 124–132. Academic Press, Boston (1992)
19. Sloane, N.J.A., Hardin, R.H., Duff, T.D.S., Conway, J.H.: Minimal-energy clusters of hard spheres. Discrete Comput. Geom. **14**(3), 237–259 (1995)
20. Smale, S.: Mathematical problems for the next century. Math. Intell. **20**(2), 7–15 (1998)
21. Sun, X., Chen, Zh.: Spherical basis functions and uniform distribution of points on spheres. J. Approx. Theory **151**(2), 186–207 (2008)

22. Tammes, P.M.L.: On the Origin of Number and Arrangement of the Places of Exit on the Surface of Pollen-Grains. Recueil des Travaux Botaniques Néerlandais, vol. 27. Koninklijke Nederlandse Botanische Vereniging (1930)
23. Teramoto, S., Asano, T., Katoh, N., Doerr, B.: Inserting points uniformly at every instance. IEICE Trans. Inf. Syst. **E89-D**(8), 2348–2356 (2006)
24. Thompson, J.J.: On the structure of the atom: an investigation of the stability and periods of oscillation of a number of corpuscles arranged at equal intervals around the circumference of a circle; with application of the results to the theory of atomic structure. Philos. Mag. **7**(39), 237–265 (1904)
25. Todhunter, I.: Spherical Trigonometry. Macmillan, London (1886)
26. Wagner, G.: On a new method for constructing good point sets on spheres. Discrete Comput. Geom. **9**(2), 111–129 (1993)
27. Yershova, A., Jain, S., Lavalle, S.M., Mitchell, J.C.: Generating uniform incremental grids on $SO(3)$ using the Hopf fibration. Int. J. Robot. Res. **29**(7), 801–812 (2010)
28. Zhang, Y., Chang, Zh., Chin, F.Y.L., Ting, H.-F., Tsin, Y.H.: Uniformly inserting points on square grid. Inf. Process. Lett. **111**(16), 773–779 (2011)
29. Zhou, R., Chen, Ch., Sun, L., Lau, F.C.M., Poon, Sh.-H., Zhang, Y.: Online uniformly inserting points on the sphere. Algorithms **11**(10), # 156 (2018)